sciendo

Polish Journal of Chemical Technology, 26, 2, 69—76, 10.2478/pjct-2024-0020

UV irradiation grafting of butyl acrylate on polyimide membrane for enhanced lubricant solvent recovery

Huilong Shi[1], Deqing Shi[1, 2*], Bowen Liu[1], Chengshuai Li[3], Hongjie Chen

[1]School of Chemical Engineering, Shandong Institute of Petroleum and Chemical Technology, Dongying, 257100, China
[2]College of Chemical Engineering, China University of Petroleum (East China), Qingdao Shandong 266580, China
[3]Shandong Academy of Pesticide Sciences, Jinan 250000, China
[*]*Corresponding author: e-mail:* shlouc@126.com

As one single membrane material could not fulfill the requests of chemical stability, mechanical strength, and resistance to pollution in practical applications. Modifications of the membrane to improve its separation performance were of great significance. In this study, UV irradiation grafting modification was employed and butyl acrylate was selected as a modification monomer for polyimide membrane to improve its lipophilicity and separation efficiency in lubricant solvent recovery. And effects of monomer concentration, irradiation distance, and grafting time on the grafting results and separation properties of modified polyimide membranes were investigated. The results exhibited that modified polyimide membranes obtained an enhanced lubricant retention rate compared with raw membranes, which increased from 66.5% to 93.1%. The industrial test for 40 days proved the great stability of modified polyimide membranes. Overall, this work confirmed the good industrial utilization potential of modified polyimide membranes and offered an effective way for lubricant solvent recovery.

Keywords: Lubricant solvent recovery, Membrane separation, Polyimide, Grafting modification, Retention rate.

INTRODUCTION

Solvent recovery was crucial to the economic and environmental benefits of lubricant manufacture. Currently, traditional technologies such as distillation and adsorption are utilized to separate lubricants and solvents[1, 2]. However, these traditional technologies limited the lubricant solvent recovery due to their shortcomings as high energy consumption, technical complexity, and poor efficiency[3, 4]. Membrane separation has attracted more and more attention owing to its advantages as no phase transition, low equipment investment, and less energy consumption[5, 6]. However, industrial applications proposed high requirements of chemical stability, mechanical strength, and resistance to pollution, which could not be fulfilled by one single membrane material[7, 8]. Modifications of the membrane to improve its separation performance were very necessary.

Membrane materials were mainly composed of organic polymers and inorganic materials at present[9, 10]. Inorganic materials such as ceramics and zeolites were rarely utilized in industrial applications due to their high costs and difficulties in manufacturing[11, 12]. Organic polymers such as polyimide, polyvinyl alcohol, and cellulose acetate were the main membrane materials for lubricant solvent recovery[13, 14]. Polyimide stood out due to its features such as great heat resistance, strong mechanical properties, and good solvent resistance[15, 16]. However, polyimide exhibited poor lipophilicity, which resulted in bad separation properties in lubricant solvent recovery[17, 18]. Therefore, surface modification to improve the lipophilicity of polyimide membrane was of great promotion for its separation performance in lubricant solvent recovery.

In this paper, butyl acrylate was utilized as a grafting monomer to modify polyimide membranes by UV irradiation grafting polymerization, which could enhance the separating property for lubricants and solvents owning to the great lipophilicity of butyl acrylate. The effects of monomer concentration, irradiation distance, and grafting time on modification results of polyimide membranes were investigated. Moreover, the separation performances of polyimide membranes modified under different conditions were evaluated with lubricant/butanone/toluene system. Furthermore, the surface chemical composition of polyimide membranes before and after modification was analyzed by attenuated total reflection infrared spectroscopy (ATR-FTIR). The cross-sectional structures of polyimide membranes were investigated by scanning electron microscope (SEM), which could obtain the structural changes of polyimide membranes before and after modification to evaluate the grafting consequences.

EXPERIMENTAL SECTION

Materials and Reagents

The used polyimide nanofiltration membranes in this paper were made in our laboratory. Petrochemical lubricants were purchased from Dalian Petrochemical Company. The butanone, toluene, anhydrous ethanol, butyl acrylate, and heptane were of analytical grade and purchased from Sinopharm Chemical Reagent Co. Ltd.

UV irradiation grafting modification of polyimide membranes

Purification of butyl acrylate

Self-polymerization reactions were prone to occur in butyl acrylate under the influence of heat and light. Thus, a certain amount of hydroquinone was required during its storage and transportation as polymerization inhibitor[19, 20]. The added hydroquinone would inhibit the polymerization of butyl acrylate and affect the grafting results. Therefore, it was necessary to refine butyl acrylate by vacuum distillation to remove the added hydroquinone. The specific processes of butyl acrylate purification were as follows. Firstly, pour a moderate amount of unpurified butyl acrylate into a three-necked flask. Then, seal the three-necked flask with ground glass stoppers and corks with a capillary tube. It should be noted that the capil-

lary tubes should be kept below the liquid level in the flask. Then connect the flexible conduit to the nitrogen cylinder, and daub vacuum ester at each junction of the device to ensure the sealing of the distillation device.

Turn on the cooling water circulation and the nitrogen cylinder switch. Then adjust the nitrogen flow rate and set the water bath temperature properly. Subsequently, start heating and vacuuming. It should be noted that the pressure of the system should be kept at 30 mmHg, and distillates at 64 °C were collected. Considering the close correlation between the boiling point of monomers and the vacuum degree, the vacuum degree should be finely controlled to ensure the stability of the distillation process. And the fraction outflow rate should be kept at –2 drops per second. When the purified butyl acrylate in the receiving bottle reaches half, turn off the vacuum pump, water bath, and nitrogen cylinder in sequence, and pour the residual liquid in the three-necked flask back into the raw material bottle. The refined butyl acrylate monomer should be sealed and stored in the refrigerator for standby.

UV irradiation grafting modification

The used polyimide membrane was a self-made polyimide nanofiltration membrane (BTDA-ODA), containing a photosensitive structure of benzophenone, which could pose polymerization reaction with olefinic monomers under UV irradiation[21, 22]. Firstly, cut out a square size of 7.0 × 7.0 cm polyimide membrane from the same batch, and wash the polyimide membrane with n-heptane. Secondly, place the polyimide membrane in an oven at 50 °C, after drying to constant weight, weigh the polyimide membrane and record it as W_0. Subsequently, measure out a certain volume of refined butyl acrylate, pour it into a clean conical flask, and then add a certain volume of n-heptane to prepare a certain concentration of grafting monomer solution.

Spread the dried polyimide membrane on the bottom of a clean watch glass. Then pour the prepared grafting monomer solution into the watch glass to make the membrane completely immersed in the solution. Then place the watch glass at a certain distance directly below the ultraviolet lamp (GGZ-1000, Shanghai Yaming Feiya Lighting Appliances Co., Ltd, 1000 W). Carry out UV irradiation grafting reaction at room temperature. After grafting for a certain time, take out the membrane, and wash the homopolymer on the membrane surface with n-heptane. Finally, put the cleaned membrane into an oven, dry it to a constant weight, then weigh the membrane and record it as W_1. The grafting outcomes could be evaluated by the grafting ratio[23, 24], which was calculated as follows.

$$D_g = (W_1 - W_0)/W_0 \times 100\% \quad (1)$$

Where W_1 was the weight of the grafted membrane, W_0 was the weight of the untreated membrane.

Characterizations

A scanning electron microscope (SEM, Hitachi S-4800) was employed to characterize the cross-sectional structures of polyimide membranes. The samples of polyimide membranes before and after modification were frozen in liquid nitrogen and then cut off to make sampling. The cross-section structures of membranes were then observed by SEM, and the changes in membrane structures before and after modification were analyzed. The changes in chemical composition and functional groups on the membrane surface before and after modification were analyzed by attenuated total reflection Fourier transform infrared spectroscopy (ATR-FTIR, NICOLET Nexus 470). It should be noted that the membrane samples should be dried in a vacuum oven at 50 °C for more than 24 hours before analysis.

Separation performance tests of membranes

The separation performance tests of polyimide membranes before and after modification were carried out on the evaluation device as shown in Figure 1. The device was divided into four parts as liquid storage system, feeding system, testing cell system, and recovery system. A liquid level indicator was installed on the storage tank to facilitate feeding. The feeding system mainly consisted of a constant flux pump, pressure gauges, and safety valves. The testing cell system consisted of three parallel membrane cells. There was a back pressure valve to regulate the system pressure downstream of the membrane cells. The recovery system sent the solvent through the back pressure valve back to the solvent tank for circulation. The prepared polyimide membranes were then utilized to separate lubricant/butanone/toluene system to investigate the effects of monomer concentration, irradiation distance, and grafting time on the separation performance of modified membranes. During the experiments, the material flow rate was kept stable at 60 mL/min, the operating pressure was kept

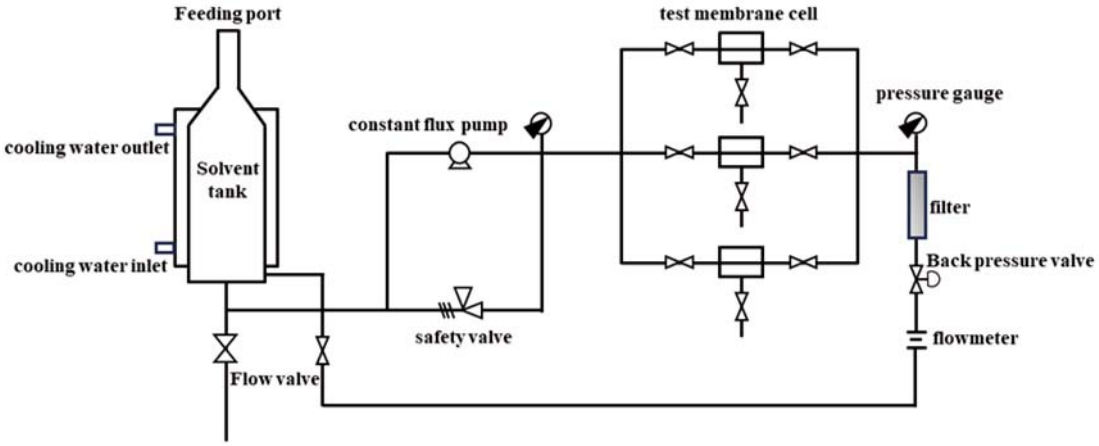


Figure 1. The equipment of membrane performance evaluation

stable at 3.0 MPa, and the lubricant concentration was kept stable at 20% (mass fraction). After 40 minutes of stable operation for the device, start sampling. Use a 5.0 mL measuring cylinder to receive the permeant at the outlet of testing cells. When the received permeant reaches a needed volume, stop sampling and record the time and permeant volume. It should be noted that three samples were taken for evaluating the separation performance of each membrane.

Liquid flux and lubricant retention rate were employed to evaluate the separating properties of membranes. Where liquid flux refers to the volume of liquid passing through the unit area of the membrane at unit time. And lubricant retention rate was the ability of membranes to prevent the passage of lubricant. Specifically, the liquid flux J and lubricant retention rate R were calculated as formulas (2) and (3)[25, 26].

$$J = \frac{V}{At} \tag{2}$$

Where J was the membrane flux ($L \cdot m^{-2} \cdot h^{-1}$), V was the volume of permeant (L), A was the area of the membrane (diameter 5.0 cm), t was time (h).

$$R = 1 - \frac{C_1}{C_0} \tag{3}$$

Where R was the lubricant retention rate, C_1 was the lubricant concentration of the permeant, C_0 was the initial lubricant concentration of the feed liquid. Additionally, the lubricant concentrations above were measured using the following gravimetric method.

Wash a medical vial thoroughly and dry it in an oven. Weigh its mass as m_1 with an accurate electronic balance, and then add a certain amount of raw material or permeant into the medical vial, weighing its weight as m_2. Put the vial containing raw material or permeant on the glass petri dish, and then put the petri dish into the heating mantle. Control the heating temperature at 100 °C to heat the solution in the vial so that the solvents can evaporate rapidly. Due to the significant difference in boiling points between lubricant and butanone/toluene, the solvents could be completely evaporated in about an hour. The lubricant was basically left in the vial, and then the vial was weighed as m_3. Subsequently, the lubricant concentration could be calculated according to the following formula (4)[27, 28].

$$C = \frac{m_3 - m_1}{m_2 - m_1} \tag{4}$$

Where C was the lubricant concentration, m_1 was the weight of the empty vial, m_2 was the weight of the empty vial and liquid, and m_3 was the weight of the empty vial and lubricant. It should be noticed that if m_3 remained unchanged before and after evaporation in the final stage of evaporation, heating could be stopped. Otherwise, heating and evaporation should continue until m_3 remains constant.

RESULTS AND DISCUSSIONS

Cross-section structure and surface composition

Cross-section structures of membranes

SEM images were employed to characterize the cross-section structures of membranes before and after modification, where the used butyl acrylate concentration was 15%, the irradiation distance was 35 cm. It could be observed from SEM images in Figure 2 that the upper surface of the polyimide membrane was a dense layer, the layer near the cortex was a sponge structure, and the basic structure of the supporting layer below was a finger-shaped pore structure[29]. There were no significant changes observed in the finger-shaped pore structure of the lower supporting layer after modification. However, it should be noticed that an apparent reduction of micropores in the dense layer of modified membranes was observed compared with raw membrane. Moreover, the surface layer and adjacent sponge structures of the modified membranes became gradually dense with the grafting time increasing, and the micropores in the dense layer became fewer and fewer. The changes

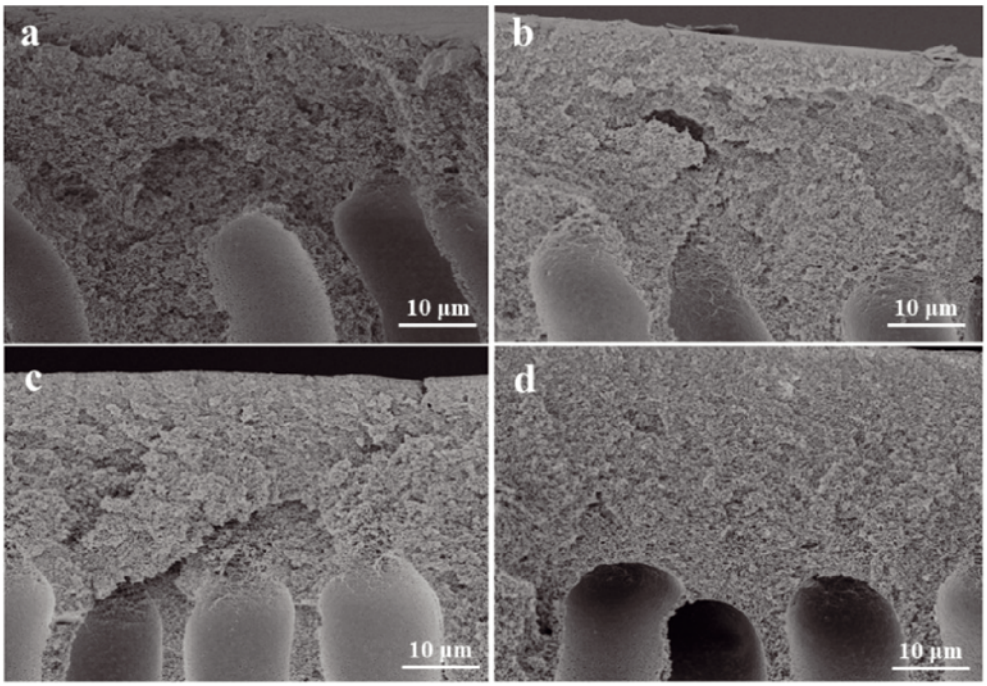


Figure 2. SEM images of polyimide membranes with different UV grafting times (a) 0 min, (b) 8 min, (c) 24 min, and (d) 40 min

in cross-section structures of membranes indicated that a grafting layer of butyl acrylate was generated on the surface and in the micropores of polyimide membranes after UV modification[30], and the quantity of butyl acrylate grafted onto polyimide membranes enlarged with grafting time increasing[31, 32].

Surface composition of membranes

ATR-FTIR spectra were utilized to analyze the surface composition of polyimide membranes before and after modification. As shown in Figure 3, clear characteristic peaks of polyimide in the infrared spectrum of all membranes were observed. Wherein, the absorption peak at 1776 cm^{-1} was an asymmetric stretching vibration peak of C=O[33]. The absorption peak at 1720 cm^{-1} was a symmetric stretching vibration peak of C=O. The absorption peak at 1380 cm^{-1} was a stretching vibration peak of C-N. Moreover, the absorption peak at 720 cm^{-1} was a bending vibration peak of C=O. It should be noticed that a new absorption peak appeared at 1205 cm^{-1}, which belonged to the stretching vibration peak of C-O-C, indicating the presence of C-O--C bonds and the grafting of butyl acrylate on polyimide membranes[34, 35]. Additionally, the peak intensity at 1205 cm^{-1} continued to increase with the grafting time growing, which illustrated that more butyl acrylate was grafted on polyimide membranes with grafting time increasing[36]. Similarly, the intensity of peaks at 1720 cm^{-1} and 720 cm^{-1} significantly enlarged with the increase of grafting time as well, which were results of more C=O functional groups provided by butyl acrylate grafted on polyimide membranes[37, 38]. The outcomes of ATR-FTIR spectra indicated that the grafting ratio of butyl acrylate on polyimide membranes increased with the extension of illumination time, which was consistent with the results of SEM analysis.

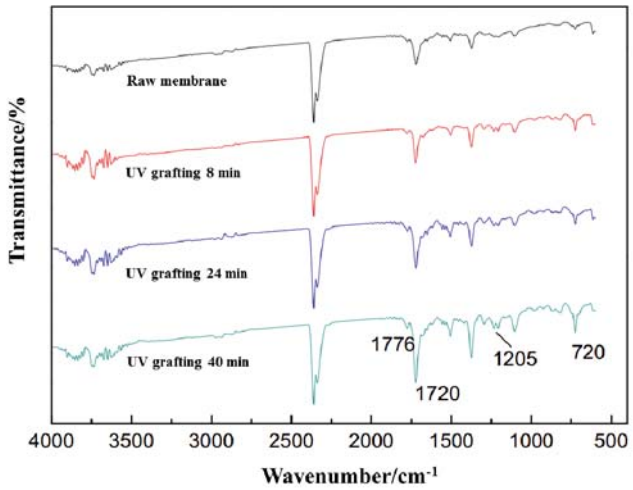


Figure 3. ATR-FTIR spectra of polyimide membranes with different UV grafting times

Grafting ratio of polyimide membranes

Effects of monomer concentration

Comparative experiments with varying butyl acrylate concentrations under conditions of constant illumination time and irradiation distance were conducted to determine the optimal concentration of grafting monomers. As shown in Figure 4, the grafting ratio of modified membranes first enlarged and then decreased with monomer concentration increasing. The main reason for the phenomenon was that the effective contact between butyl acrylate and polyimide membranes improved significantly with the concentration of butyl acrylate increasing, which led to the continuous increase of grafting ratio[39, 40]. However, the serious self-polymerization reactions of butyl acrylate as its concentration increased ulteriorly inhibited the grafting reaction, which eventually resulted in the decrease of the grafting ratio[41]. Consequently, it could be concluded that the optimal concentration of grafting monomers was 15%, and the highest grafting ratio of 1.36% was reached.

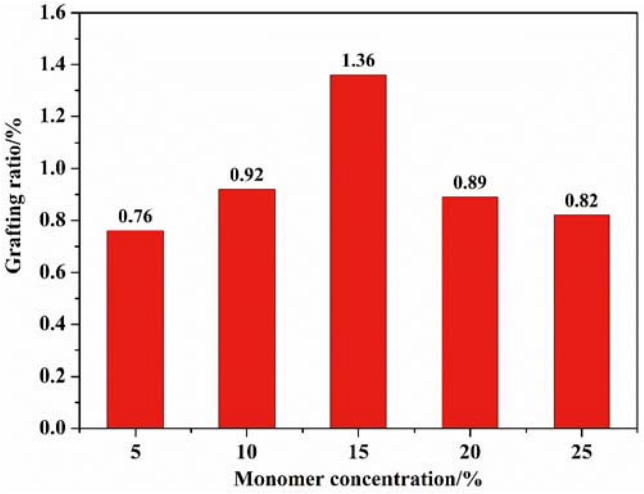


Figure 4. Effects of monomer concentrations on grafting ratio

Effects of irradiation distance

As grafting reactions of butyl acrylate on polyimide membranes were induced by UV irradiation, the irradiation distance displayed a significant impact on the grafting ratio. Herein, the effects of irradiation distance on the grafting ratio of modified membranes were investigated with a monomer concentration of 15% under constant illumination time. As shown in Figure 5, the grafting ratio of modified polyimide membranes improved firstly and then remained unchanged with irradiation distance decreasing. The main reason for the phenomenon was that the UV irradiation intensity increased with the irradiation distance decreasing. The increased irradiation intensity could produce more radicals on polyimide membranes, which ultimately led to more butyl acrylate grafted on membranes, and the grafting ratio of the mo-

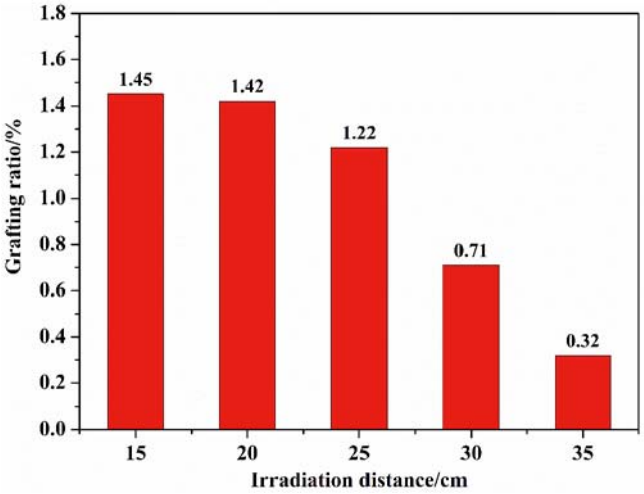


Figure 5. Effects of irradiation distances on grafting ratio

dified membrane improved correspondingly[42]. However, it should be noticed that limited contact between butyl acrylate and polyimide membranes hindered the further increase of the grafting ratio, which resulted in the unchanged grafting ratio even if the irradiation distance was further reduced. Additionally, the mechanical strength of polyimide membranes would be damaged when the ultraviolet lamp was placed to close[43]. Consequently, the optimal irradiation distance was 20 cm, and the superior grafting ratio of 1.42% was reached.

Effects of grafting time

Grafting time affected the grafting ratio, and displayed significant impacts on the production costs of grafting modification as well. Hence, comparative experiments with varying grafting time under butyl acrylate concentration as 15% and irradiation distance of 20 cm were carried out to investigate the effects of grafting time. As shown in Figure 6, the grafting ratio of modified membranes improved firstly and then kept basically unchanged with illumination time increasing. The main reason for the phenomenon was that more photosensitive groups of benzophenone on polyimide membranes reacted with butyl acrylate as time prolonged, which led to more butyl acrylate grafted on membranes[44]. However, it should be noted that the butyl acrylate layer on the membrane surface would inhibit the subsequent grafting process. The excessive grafting time would increase the costs of grafting modification[45]. Consequently, the optimal grafting time was 40 min under comprehensive consideration of the grafting ratio and process costs, the superior grafting ratio of 1.38% was reached.

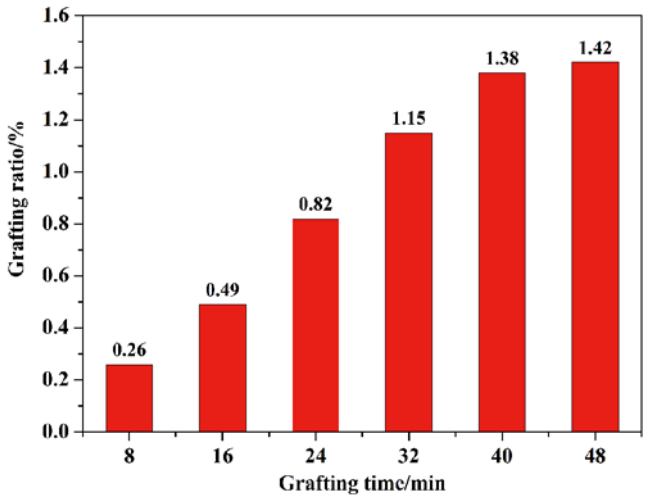


Figure 6. Effects of grafting time on grafting ratio

Separation property of modified polyimide membranes

Effects of monomer concentration

Effects of monomer concentration on the separation property of modified polyimide membranes were investigated with lubricant/butanone/toluene system. As shown in Figure 7, the retention rate of lubricant improved to 93.8% from 66.5% firstly, then decreased to 86.1%. Meanwhile, the flux decreased to 5.52 L/($m^2 \cdot h$) *from 14.0 L/($m^2 \cdot h$), and then* enlarged to 7.41 L/($m^2 \cdot h$) *as the butyl acrylate concentration increased from 0% to 25%.* The main reason for the phenomenon was that more butyl acrylate was grafted on modified polyimide membranes as monomer concentration increased from 0% to 15%, which led to fewer pore structures on the surface of modified membranes. The denser surface would ultimately improve the retention rate of lubricant and diminish the flux[46]. However, it should be noted that excessive butyl acrylate would result in a serious self-polymerization reaction, which eventually caused a decrease in retention rate and an increase in flux. Moreover, the average flux of modified polyimide membranes exhibited an opposite changing trend compared with the retention rate, as the fewer pore structures of membranes caused by the increased grafting rate would diminish the average flux[47]. The lower grafting rate indicated more pore structures on the surface of modified membranes, which were conducive to the improvement of average flux. Comprehensive consideration of the effects of monomer concentration on average retention rate and flux, it could be concluded that 15% was the optimal grafting concentration for butyl acrylate and the retention rate of lubricant as 93.8% as well as the flux was 5.52 L/($m^2 \cdot h$) were reached.

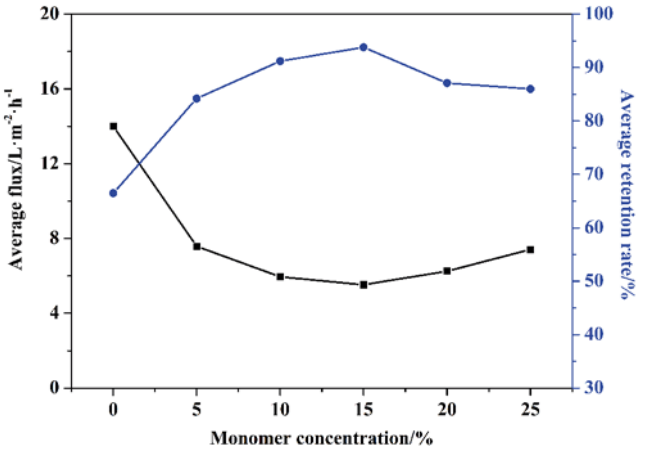


Figure 7. Effects of monomer concentration on separation property of modified polyimide membranes

Effects of irradiation distance

Effects of irradiation distance on the separation property of modified polyimide membranes were investigated with a monomer concentration of 15%. As shown in Fig. 8, the retention rate of the lubricant kept diminishing and the flux kept increasing with the irradiation distance

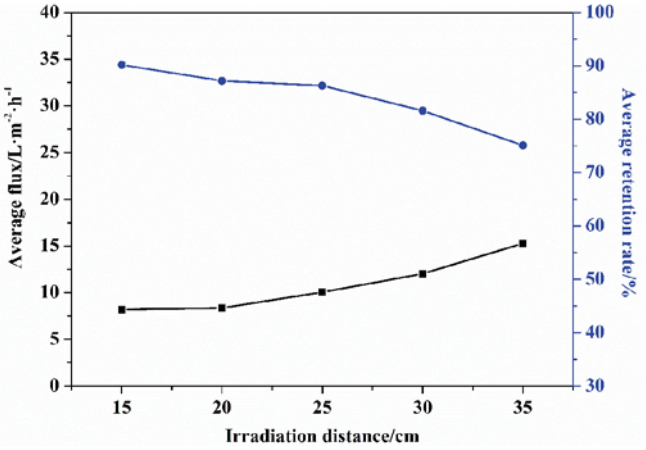


Figure 8. Effects of irradiation distance on separation property of modified polyimide membranes

enlarging. The main causes of the phenomenon were that the grafting ratio declined with the irradiation distance enlarging, which led to less butyl acrylate grafted on modified membranes, and eventually resulted in fewer pore structures in modified membranes[48]. The loose membrane surface was conducive to the enlargement of the flux. However, the loose membrane surface would result in the diminishment of the retention rate[49]. As the retention rate for lubricant and the flux of organic solvent were both important to the separation property of modified polyimide membranes, the optimal irradiation distance was 25 cm by comprehensive considerations. The retention rate for lubricant of 86.3% as well as the flux of 10.05 L/($m^2 \cdot h$) were reached.

Effects of grafting time

Effects of grafting time on the separation property of modified polyimide membranes were investigated with a monomer concentration of 15% and irradiation distance of 25 cm. As shown in Figure 9, the retention rate for lubricant kept increasing and the flux kept diminishing with the grafting time extending. The effects of grafting time on the retention rate for lubricant and the flux of organic solvent were the opposite. The main causes of this phenomenon were that more butyl acrylate was grafted on modified membranes with the grafting time extending, which led to fewer pore structures in modified membranes[50]. The dense surface structure of modified membranes would enhance the retention rate for lubricant and diminish the flux of organic solvent[51]. As the retention rate for lubricant and the flux of organic solvent were both important for the separation property of modified polyimide membranes, the appropriate grafting time was determined as 40 min. The retention rate for lubricant of 93.1% as well as the flux of 5.18 L/($m^2 \cdot h$) were reached.

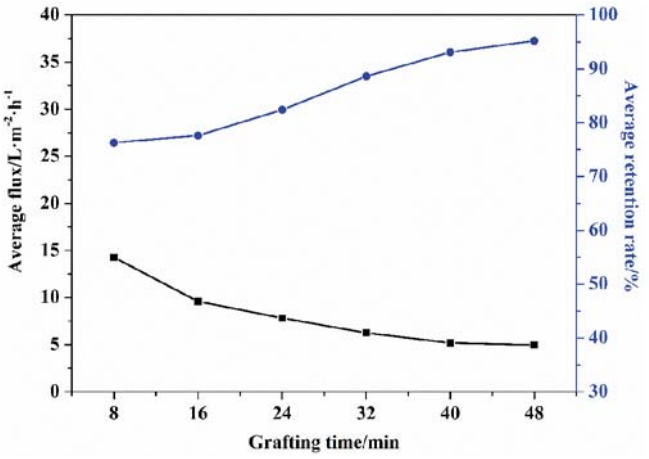


Figure 9. Effects of grafting time on separation property of modified polyimide membranes

Industrial test of modified polyimide membranes

An industrial test lasting for 40 days at 3.0 MPa was implemented to investigate the stability performance of modified polyimide membranes. The industrial test was conducted with a monomer concentration of 15%, irradiation distance of 25 cm, and grafting time of 40 min. As shown in Fig. 10, the optimal retention rate reached 96.2% on the fourth day, the minimal optimal retention rate was 93.1% on the 29th day, and the average retention rate for lubricant was 94.03% during the whole industrial test. Additionally, the optimal flux was achieved as 12.36 L/($m^2 \cdot h$) on the 7th day, the minimal flux was 6.81 L/($m^2 \cdot h$) on the 31st day, and the average flux of organic solvent was 9.23 L/($m^2 \cdot h$) in the industrial test. It should be noted that the modified polyimide membranes obtained superior separating properties for lubricant solvent recovery compared with the lab-scale experiment, it was mainly owning to the better process control in the industrial test[52]. Moreover, it could be concluded that the retention rate for lubricant and the flux of organic solvent both remained stable during the 40 days of industrial test, which indicated the great industrial application potential of modified polyimide membranes.

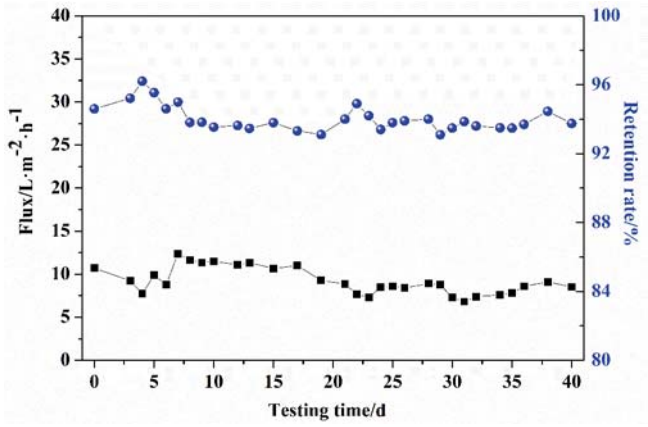


Figure 10. Industrial test of modified polyimide membranes

CONCLUSIONS

In this paper, UV irradiation grafting method was employed to modify polyimide membranes using butyl acrylate as a grafting monomer to enhance the lubricant solvent recovery. The results indicated that grafting butyl acrylate on polyimide membranes could boost the efficiency of lubricant solvent recovery. The SEM and ATR-FTIR analysis indicated that grafting butyl acrylate on polyimide membranes reduced the pore structures in membranes, which ultimately improved the retention rate for lubricant and diminish the flux of organic solvent. As the retention rate and the flux were both important for lubricant solvent recovery, the experimental conditions were optimized with comprehensive considerations. The retention rate for lubricant of 93.1% and the flux of 5.18 L/($m^2 \cdot h$) were achieved. Furthermore, the industrial test proved the great stability performance of modified polyimide membranes, which indicated their good industrial utilization potential. Our work confirmed the good industrial utilization potential of modified polyimide membranes and offered an effective way for lubricant solvent recovery.

Declaration of Competing Interest

There are no conflicts to declare.

Acknowledgments

This study was supported by the Science Development Fund Project of Dongying City (No.: DJ2020027).

LITERATURE CITED

1. Yuan, B., Cao, M., Sun, H., Wang, T., Bu, X., Shi, D., Kong, Y. & Li, P. (2014). Preparation of a Polyimide Nanofiltration Membrane for Lubricant Solvent Recovery. *J. Appl. Polymer Sci.* 131(15) 1–8. DOI:10.1002/40338.

2. Baig, U., Faiza, M.N. & Dastageer, M. (2021). Polyimide based super-wettable membranes/materials for high performance oil/water mixture and emulsion separation: A review. *Adv. Colloid Interf. Sci*. 297, 102525. DOI: 10.1016/j.cis.2021.102525.

3. Firman, L.R., Ochoa, N.A., Marchese, J. & Pagliero, C.L. (2013). Deacidification and solvent recovery of soybean oil by nanofiltration membranes. *J. Membrane Sci.* 431, 187–196. DOI: 10.1016/j.memsci.2012.12.040.

4. Favvas, E.P., Katsaros, F.K., Papageorgiou, S.K., Sapalidis, A.A. & Mitropoulos, A.C. (2017). A review of the latest development of polyimide based membranes for CO_2 separations. *React. Functional Polym.* 120, 104–130. DOI: 10.1016/j.reactfunctpolym.2017.09.002.

5. Zhu, H., Chen, K., Sun, G., Zhao, W., Jiang, Q. & Xiao, C. (2023). Robust design of durable PTFE/graphene hollow fiber composite membrane for high-temperature lubricant recycling. *J. Water Proc. Engin.* 55, 1–10. DOI: 10.1016/j.jwpe.2023.104163.

6. Liu, M., Shen, L., Wang, J., Ding, Y., Zhou, Y. & Liu, F. (2022). Continuous separation and recovery of high viscosity oil from oil-in-water emulsion through nondispersive solvent extraction using hydrophobic nanofibrous poly(vinylidene fluoride) membrane. *J. Membrane Sci.* 660, 1–8. DOI: 10.1016/j.memsci.2022.120876.

7. Tanudjaja, H.J., Hejase, C.A., Tarabara, V.V., Fane, A.G. & Chew, J.W. (2019). Membrane-based separation for oily wastewater: A practical perspective. *Water Res.* 156, 347–365. DOI: 10.1016/j.watres.2019.03.021.

8. Palanisamy, T., Tabatabai, S., Zhang, T. & Leiknes, T. (2021). Role of surfactants in cleaning of PVDF ultrafiltration membranes fouled by emulsified cutting oil. *J. Water Process Engin.* 40, 1–9. DOI: 10.1016/j.jwpe.2021.101923.

9. Nadeem, A.K., Awais, B., Muhammad, M., Jiří, J.K., Rachida, E., Roohul, A.K., Majed, A., Mudassar, A., Sidra, S., Ahmad, M., Apurav, K. & Pau, L.S. (2022). Treatment of Hospital wastewater with submerged aerobic fixed film reactor coupled with tube-settler. *Chemosphere,* 286. DOI: 10.1016/j.chemosphere.2021.131838.

10. Alsubih, M., morabet, R.E., Khan, R.A., Khan, N., Khan, A. & Sharma, G. (2021). Performance evaluation of aerobic fluidized bed bioreactor coupled with tube-settler for hospital wastewater treatment. *J. Environ. Chem. Engin.* 9(5). DOI: 10.1016/j.jece.2021.105896.

11. Saadati, J. & Pakizeh, M. (2017). Separation of oil/water emulsion using a new PSf/pebax/F-MWCNT nanocomposite membrane. *J. Taiwan Instit. Chem. Engin.* 71, 265–276. DOI: 10.1016/j.jtice.2016.12.024.

12. Rouquié, C., Szymczyk, A., Rabiller-Baudry, M., Roberge, H., Abellán, P., Riaublanc, A., Frappart, M., Álvarez-Blanco, S. & Couallier, E. (2022). NaCl precleaning of microfiltration membranes fouled with oil-in-water emulsions: Impact on fouling dislodgment. *Separ. Purific. Technol. 285*, 1–14. DOI: 10.1016/j.seppur.2021.120353.

13. Xin, Y. & Yin, F. (2021). A combined experimental and molecular simulation study of lube oil dewaxing solvent recovery using membrane. *Separ. Purific. Technol.* 261, 1–12. DOI: 10.1016/j.seppur.2020.118278.

14. Liu, Y., Sun, W., Feng, K., Wu, Y., Yu, B., Liu, S. & Zhou, F. (2023). Sebaceous gland-inspired self-lubricated de-icing coating by continuously secreting lubricants. *Progress in Organic Coatings*, 174, 1–7. DOI: 10.1016/j.porgcoat.2022.107311.

15. Huang, Y., Xu, M., Guo, Q., Xie, W., Shu, J., Du, X., Qiu, F., Huang, S. & Huang, Q. (2023). A robust and environmental-friendly strategy for preparation of PTFE membranes with high separation accuracy and sequential separation performance. *J. Environ. Chem. Engin.* 11(3), 1–14. DOI:10.1016/j.jece.2023.110310.

16. Dmitrenko, M., Kuzminova, A., Zolotarev, A., Markelov, D., Komolkin, A., Loginova, E., Plisko, T., Burts, K., Bildyukevich, A. & Penkova, A. (2022). Modification strategies of polyacrylonitrile ultrafiltration membrane using TiO_2 for enhanced antifouling performance in water treatment. *Separ. Purific. Technol.* 286, 1–13. DOI: 10.1016/j.seppur.2022.120500.

17. Gan, G., Fan, S,. Li, X., Zhang, Z. & Hao, Z. (2023). Adsorption and membrane separation for removal and recovery of volatile organic compounds. *J. Environ. Sci. (China)*, 123, 96–115. DOI:10.1016/j.jes.2022.02.006.

18. Huang, T.Y., Jia, S.H., Goh, S. & Chong, T.H. (2021). Ethanol recovery from dilute aqueous solution by perstraction using supported ionic liquid membrane (SILM). *J. Cleaner Produc. 298*, 1–10. DOI: 10.1016/j.jclepro.2021.126811.

19. Sawatdiruk, S., Charoensuppanimit, P., Faungnawakij, K. & Klaysom, C. (2021). POSS/PDMS composite pervaporation membranes for furfural recovery. *Separ. Purific. Technol.*, 278, 1-10. DOI: 10.1016/J.SEPPUR.2021.119281.

20. Singh, P., Manikandan, N., Purnima, M., Pakshirajan, K. & Pugazhenthi, G. (2020). Recovery of lignin from water and methanol using low-cost kaolin based tubular ceramic membrane. *J. Water Proc. Engin.* 38, 1–11. DOI: 10.1016/J.JWPE.2020.101615.

21. Tashvigh, A. & Chung, T.S. (2019). Robust polybenzimidazole (PBI) hollow fiber membranes for organic solvent nanofiltration. *J. Membrane Sci.* 572, 580–587. DOI: 10.1016/j.memsci.2018.11.048.

22. Koncsag, C. & Kirwan, K. (2012). A membrane screening for the separation/concentration of dilignols and trilignols from solvent extracts. *Separ. Purific. Technol.* 94, 54–60. DOI: 10.1016/J.SEPPUR.2012.04.009.

23. Paseta, L., Luque-Alled, J.M., Malankowska, M., Navarro, M. & Téllez, C. (2020). Functionalized graphene-based polyamide thin film nanocomposite membranes for organic solvent nanofiltration. *Separ. Purific. Technol.* 247, 1–9. DOI: 10.1016/j.seppur.2020.116995.

24. Zhang, Y., Xu, P., Chen, X., Qiu, M. & Fan, Y. (2022). Preparation of high permeance thin-film composite nanofiltration membrane on macroporous ceramic support. *J. Membrane Sci.*, 663, 1–11. DOI: 10.1016/j.memsci.2022.121076.

25. Yu, Q., Zhu, J., Gong, G., Yu, L., Hu, Y. & Li, J. (2023). Efficient preparation of ultrathin ceramic wafer membranes for the high-effective treatment of the oilfield produced water. *Separ. Purific. Technol.* 308 1–13. DOI: 10.1016/j.seppur.2022.122720.

26. Suárez, L., Diez, MA., García, R. & Riera, FA. (2012). Membrane technology for the recovery of detergent compounds: A review. *J. Ind. Engin. Chem. 18*, (6), 1859–1873. DOI: 10.1016/J.JIEC.2012.05.015.

27. Dashtbozorg, A., Saljoughi, E., Mousavi, S.M. & Kiani, S. (2022). High-performance and robust polysulfone nanocomposite membrane containing 2D functionalized MXene nanosheets for the nanofiltration of salt and dye solutions. *Desalination*, 527, 1–13. DOI: 10.1016/j.desal.2022.115600.

28. Fu, W., Liu, Y., Liu, J., Zhang, B., Cheng, J., Du, R., Sun, M., Zhao, Y. & Che, L. (2023). A TiO_2 modified whisker mullite hollow fiber ceramic membrane for high-efficiency oil/water emulsions separation. *J. European Ceramic Soc.* 43(10), 4451–4461. DOI: 10.1016/j.jeurceramsoc.2023.03.029.

29. Silva, A., Silva, J.D., Vicente, R., Ambrosi, A., Zin, G., Luccio, M.D. & Oliveira, Jd. (2023). Recent advances in surface modification using polydopamine for the development of photocatalytic membranes for oily wastewater treatment. *J. Water Proc. Engin. 53*, 1-20. DOI: 10.1016/j.jwpe.2023.103743.

30. Obidara, T., Azeem, M., Lawal, D., Alfaraj, M., Abdulhamid, M. & Baroud, T. (2023). Novel hexa-fluorinated intrinsically porous polyimide membranes for the desalination

of high saline water by air-gap membrane distillation. *Desalination*, 566. DOI: 10.1016/j.desal.2023.116948.

31.Arefi-Oskoui, S., Khataee, A., Safarpour, M. & Vatanpour, V. (2020). Modification of polyethersulfone ultrafiltration membrane using ultrasonic-assisted functionalized MoS_2 for treatment of oil refinery wastewater. *Separ. Purific. Technol.* 238, 1–13. DOI: 10.1016/j.seppur.2019.116495.

32. Li, W., Musa, DAR., Ahmad, N., Adil, M., Altimari, U.S., Ibrahim, A.K., Alshehri, A.M., Riyahi, Y., Jaber, A.S., Kadhim, SI., Rushchitc, A. & Aljuaid, M.O. (2023). Comprehensive review on the efficiency of ionic liquid materials for membrane separation and environmental applications. *Chemosphere*, 332, 138826–138835. DOI: 10.1016/j.chemosphere.2023.138826.

33. Gu, Y., Zhang, B., Fu, Z., Li, J., Yu, M., Li, L. & Li, J. (2021). Poly (vinyl alcohol) modification of poly (vinylidene fluoride) microfiltration membranes for oil/water emulsion separation via an unconventional radiation method. *J. Membrane Sci.* 619, 1–10. DOI: 10.1016/J.MEMSCI.2020.118792.

34. Kayanja, O., Hassan, M.A., Hassanin, A., Ohashi, H. & Khalil, A. (2023). Effect of phase disparity of MoS_2 nanosheets on the performance of PES membranes for dual industrial oil-in-water emulsion separation and dyes adsorption. *Process Safety Environ. Protec.* 171, 55–70. DOI: 10.1016/j.psep.2023.01.014.

35. Liu, D., Cao, J., Qiu, M., Zhang, G. & Hong, Y. (2022). Enhanced properties of PVDF nanofibrous membrane with liquid-like coating for membrane distillation. *Separ. Purific. Technol.* 295, 1–10. DOI: 10.2139/ssrn.4002098.

36. Zhuge, Y. & Liu, F. (2023). Controlled preparation of polyimide/polysulfone amide (PI/PSA) porous micro-nano fiber membranes by microemulsion electrospinning for excellent thermal insulation. *Europ. Polymer J.* 194. DOI: 10.1016/j.eurpolymj.2023.112170.

37. Abdulhamid, M.A. & Muzamil, K. (2023). Recent progress on electrospun nanofibrous polymer membranes for water and air purification: A review. *Chemosphere*, 310, 136886–136907. DOI: 10.1016/j.chemosphere.2022.136886.

38. Feng, X., Yu, Z., Long, R., Sun, Y., Wang, M., Li, X. & Zeng, G. (2020). Polydopamine intimate contacted two-dimensional/two-dimensional ultrathin nylon basement membrane supported RGO/PDA/MXene composite material for oil-water separation and dye removal. *Separ. Purific. Technol.* 247, 1–16. DOI: 10.1016/j.seppur.2020.116945.

39. Hubadillah, S.K., Jamalludin, M.R., Dzarfan, O.M.H. & Iwamoto, Y. (2022). Recent progress on low-cost ceramic membrane for water and wastewater treatment. *Ceramics Internat.* 48 (17), 24157–24191. DOI: 10.1016/j.ceramint.2022.05.255.

40. Bessa, L.P., Ferreira, E.D.P., Cardoso, V.L., Reis, M.H.M. (2022). Air-sintered silicon (Si)-bonded silicon carbide (SiC) hollow fiber membranes for oil/water separation. *J. Europ. Ceramic Soc.* 42 (2), 402–411. DOI: 10.1016/j.jeurceramsoc.2021.08.025.

41. Ye, Z., Wang, L., Sun, W., Hu, Y. & Tang, H. (2020). Membrane technologies for Li^+/Mg^{2+} separation from salt-lake brines and seawater: A comprehensive review. *J. Ind. Engin. Chem.* 81, 7–23. DOI: 10.1016/j.jiec.2019.09.002.

42. Ihsanullah, I. & Bilal, M. (2022). Recent advances in the development of MXene-based membranes for oil/water separation: A critical review. *Appl. Mater. Today*, *29*, 1–18. DOI: 10.1016/j.apmt.2022.101674.

43. Zuo, C., Wang, L., Tong, Y., Shi, L., Ding, W. & Li, W. (2021). Co-deposition of pyrogallol/polyethyleneimine on polymer membranes for highly efficient treatment of oil-in-water emulsion. *Separ. Purific. Technol.* 267, 1–11. DOI: 10.1016/J.SEPPUR.2021.118660.

44. Ullah, A., Tanudjaja, H.J., Ouda, M., Hasan, S. & Chew, J. (2021). Membrane fouling mitigation techniques for oily wastewater: A short review. *J. Water Proc. Engin.* 43, 1–14. DOI: 10.1016/j.jwpe.2021.102293.

45. Hu, C., Fang, J., Jeng, R., Wu, C., Huang, Y., Sun, Y., Le, Ke. & Lai, J. (2023). Construction of transfer-free regular through-pore polyimide composite microfiltration membranes via amphiphilic dendron-assisted breath-figure method for water treatment. *Separ. Purific. Technol.* 327. DOI: 10.1016/j.seppur.2023.124981.

46. Liu, L., Liu, S., Wang, E., Dong, Q., Li, H. & Su, B. (2024). Constructing a tannic-Fe interlayer via a simple in-situ method to enhance the filtration performance of hollow fiber organic solvent nanofiltration membranes. *J. Membrane Sci.* 691. DOI: 10.1016/j.memsci.2023.122250.

47. Salahi, A., Mohammadi, T., Behbahani, R. & Hemmati, M. (2015). Asymmetric polyethersulfone ultrafiltration membranes for oily wastewater treatment: Synthesis, characterization, ANFIS modeling, and performance. *J. Environ. Chem. Engin.* 3(1), 170–178. DOI:10.1016/J.JECE.2014.10.021.

48. Fang, Y., Zhu, C., Yang, H., Zhang, C. & Xu, Z. (2024). Polyamide nanofiltration membranes by vacuum-assisted interfacial polymerization: Broad universality of Substrate, wide window of monomer concentration and high reproducibility of performance. *J. Colloid Interf. Sci.* 655, 327–334. DOI: 10.1016/j.jcis.2023.11.002.

49. Hazarika, B., Ahmaruzzaman, M., Santosh, M.S., Barceló, D. & Rtimi, S. (2023). Advances in polymer-based nanocomposite membranes for water remediation: Preparation methods, critical issues and mechanisms. *J. Environ. Chemical Engin.* 11(6). DOI: 10.1016/j.jece.2023.111401.

50. Cui, Y. & Chung, T. (2018). Pharmaceutical concentration using organic solvent forward osmosis for solvent recovery. *Nature Commun.* 9(1), 1–8. DOI: 10.1038/s41467-018-03612-2.

51. Gong, X., Zhang, L., Liu, Y. & Zhu, M. (2023). A review on zeolitic imidazolate framework-8 based materials with special wettability for oil/water separation. *J. Environ. Chem. Engin.* 11 (6). DOI: 10.1016/j.jece.2023.111360.

52. Pham, Q., Goudeli, E. & Scholes, C. (2023). Selective separation of water and methanol from hydrogen and carbon dioxide at elevated temperature through polyimide and polyimidazole based membranes. *J. Membrane Sci.* 686. DOI: 10.1016/j.memsci.2023.121990.